MINERALOGIC MAPPING USING AIRBORNE VISIBLE INFRARED IMAGING SPECTROMETER (AVIRIS) SHORTWAVE INFRARED (SWIR) DATA ACQUIRED OVER CUPRITE, NEVADA

SIMON J. HOOK, Jet Propulsion Laboratory, California Institute of Technology, Pasadena, California, and
MICHAEL RAST, European Space Agency, Noorwijk, The Netherlands.

ABSTRACT

This paper evaluates the use of AVIRIS SWIR data acquired in 1989 for discriminating and identifying alteration minerals at Cuprite, Nevada.

Initially, the AVIRIS data were processed by a variety of scene-based techniques in order to determine the optimum methodology for identifying several areas of known mineralogy on the basis of the location of diagnostic spectral absorption features. These techniques included the decorrelation stretch, log residuals, flat-field correction, hull quotients/differences, and wavelength-depth, full-width-half-maximum (WDW) images. Of these, the decorrelation stretch, log residual, and WDW images proved most effective for delineating the areas of known alteration mineralogy. These data were used to produce a mineralogic map of the area that divided the alteration into zones dominated by the minerals alunite, kaolinite, buddingtonite, and silica, respectively. This map was checked by comparison with existing geologic maps, field mapping and X-Ray Diffraction (XRD), and laboratory spectral analysis of field samples.

In general, the mineralogic map concurred with an existing alteration map that had divided the alteration into argillised, opalised, and silicified zones. The area covered by the combined alunite and kaolinite zones corresponded to area covered by the argillised and opalised zones. The silicified zone of the mineralogic map matched the silicified zone of the alteration map and was divided further into an outer and inner silicified zone.

INTRODUCTION

The wavelength region between 2000 and 2400 nm in the SWIR is particularly useful for mineralogic mapping studies, because it contains a large number of absorption features diagnostic of the presence of certain hydroxyl- and carbonate-bearing minerals or mineral groups (Goetz et al. 1983).

In this paper we evaluate the mineral discrimination and identification capabilities of the 1989 AVIRIS data covering the 2000- to 2400-nm wavelength range. The approach used for this evaluation involved processing the AVIRIS data with several scene-based techniques developed to enhance the diagnostic absorption features of a variety of alteration minerals.

These included the decorrelation stretch, flat-field correction, log residuals, hull quotients/differences, and WDW. These procedures were selected because they do not require external data such as reflectance spectra of calibration targets or estimates of incoming solar irradiances.

STUDY SITE

The Cuprite area is located on the western edge of Esmeralda County, Nevada, about 25 kilometers south of the town of Goldfield. The study area is divided in half by U.S. Highway 95 (Figure 1). On the west side of the highway the

geology exposed consists of Cambrian sediments and metasediments, Tertiary volcanics, and Quaternary alluvium. On the eastern side of the highway only the Tertiary volcanics and Quaternary alluvium have been mapped (Figure 1).

Sections of the Tertiary volcanics on both sides of the highway were intensively altered in mid- to late-Miocene times. Ashley and Abrams (1980) divided the alteration into three field-mappable zones; silicified rocks, opalized rocks, and argillised rocks (Figure 2). The alteration on the east side of the highway has a bullseye pattern, with the silicified zone forming a circular core surrounded by opalised then argillised rocks (Figure 2). The minerals identified in these alteration zones by Ashley and Abrams (1980) include quartz, opaline silica, alunite, kaolinite, and calcite.

The distribution of these alteration assemblages is typical of a fossilised hot-spring deposit (e.g. Buchanan et al. 1981). The recognition of such deposits is particularly important for mineral exploration since they frequently contain economic gold mineralisation.

In addition to the minerals described, buddingtonite (an ammonium feldspar) has been identified at Cuprite using high spectral resolution data from the 2000- to 2400-nm wavelength range in a study by Goetz and Srivastava (1985). This mineral has also been shown to be associated with gold-bearing fossilised hot-spring deposits (Krohn and Altaner, 1987).

The wealth of alteration minerals present at Cuprite coupled with the excellent exposure, limited soil development and sparse vegetation cover (0 to 10%) has led to Cuprite becoming a major testing area for evaluating the mineralogic mapping capabilities of airborne and spaceborne sensors. These include studies using data from the first airborne imaging spectrometer (Goetz and Srivastava 1985) and more recently data from the Geophysical Environmental Research Imaging Spectrometer (Kruse et al. 1990).

DATA PROCESSING AND INTERPRETATION

Initially, three bands were selected from the AVIRIS data which, based on known mineral absorption features, would separate the minerals alunite, buddingtonite, and kaolinite. These were AVIRIS bands 187 (2088 nm), 192 (2134 nm), and 198 (2217 nm). These three bands were processed with the decorrelation stretch algorithm and then displayed as red, green and blue, respectively, to form a false-color composite (Figure 3/Slide 20). The decorrelation stretch technique is described in Gillespie et al. (1986), and enhances reflectance variations whilst retaining topographic information useful for spatial orientation.

This false-color composite permits discrimination of many of the mapped lithologies and also alteration types (Figure 3/Slide 20, Figures 1 and 2). Areas of alunite appear magenta; buddingtonite, deep blue; and kaolinite, yellow. The area mapped as the silicified zone varies in color from an inner core, light blue in color, to an outer rim, green in color. For applications where the composition of the ground is known at selected locations, a product similar to that shown in Slide 20 provides an excellent tool for discriminating lithologies and alteration zones. However, in order to fully utilize all the channels of data available, a series of systematic effects unrelated to the composition of the terrain surface need to be removed: in particular, the solar irradiance curve, atmospheric attenuation/ scatter, and topographically induced illumination differences. These effects often mask subtle absorption features that can be used to identify certain alteration minerals through comparison with laboratory spectra of known minerals. A variety of techniques have been developed to remove some or all of these effects.

They include flat-field correction (Roberts et al. 1986), internal average reflectance (Kruse et al. 1988), log residuals, and hull quotients/differences (Green and Craig 1985).

The techniques examined in this study were the flat-field correction, log residuals, and hull quotients/differences. Of these, log residuals proved the most effective method, on the basis that it recovered the spectral shapes for several areas of known mineralogy and introduced the least number of artifacts into the data. Five spectra were extracted from the log residual data, which illustrate some of the absorption features of the alteration minerals present at this site (Figure 4). These spectra are mean spectra calculated from a box of pixels that appeared the same color on the decorrelation stretch images. The size of the extracted boxes depends on how large the area with a distinct color appeared on the image. For example, the largest box extracted was from the alunite area (312 pixels) and the smallest box extracted was from the buddingtonite area (12 pixels). The location of these boxes is shown on Figure 3/Slide 20 and numbered 1 through 5. The dashed lines either side of the mean spectra are the mean +/- 1 standard deviation. Also shown, are laboratory spectra from the weathered surfaces of field samples collected from these five areas. The laboratory spectra were obtained with a Beckman UV-5240 Spectrophotometer equipped with an integrating sphere. The Beckman has bands every 4 nm in 2000- to 2400-nm wavelength region with bandwidths from 20 to 28 nm.

The location and shape of absorption features in the laboratory spectra closely match those in the corresponding image log residual spectra. Particularly noteworthy in the image spectra is the detection of the kaolinite doublet between 2160 nm and 2250 nm (Figure 4). The mineral dickite has a similar doublet with a slightly different shape. The ability to detect this doublet may enable separation of areas dominated by kaolinite from those dominated by dickite. This is particularly important for mineral exploration since kaolinite can result from weathering by authigenesis in sediments or by hydrothermal processes, whereas dickite typically results from hydrothermal processes (Murray, 1988). The asymmetry in the alunite laboratory spectrum around 2200 nm is less apparent in the log residual spectrum from the same area. Isolated pixels were located in which the doublet was well defined; the loss of this feature in the mean spectrum from the larger area may result from spectral mixing with other alteration minerals.

The image spectra from the silicified zone exhibit a strong absorption feature around 2250 nm. An absorption feature at this wavelength has been noted in hydrothermal silica collected from Nevada and Utah (Podwysocki et al. 1985). These workers attribute this absorption to "gel effects", or noncrystalline silica. This absorption may also result, in part, from the log residual calculation, which involves subtracting off the log mean of each band from the log of each pixel in that band. If this mean is dominated by an absorption feature around 2200 nm, then any spectra not containing an absorption feature at this wavelength would be artificially elevated giving the appearance of a drop-off at longer wavelengths. The color difference between the inner and outer silicified zone appears to relate to the steepness of the slope from shorter wavelengths to the absorption at 2250 nm.

Using this approach, of taking an area of uniform color in the decorrelation stretch image and extracting an average log residual spectrum, it was possible to begin to produce a simplified alteration map of the area. However, numerous ambiguities arose where it was difficult to assign an area to a dominant alteration mineral. Therefore, a further technique was developed that involved examining the wavelength, depth, and full width half maximum (WDW) of the deepest absorption feature. Prior to searching for this feature, it is necessary to remove any atmospheric absorptions, otherwise the deepest absorption feature detected will frequently relate to the atmosphere rather than the composition of the surface. In addition, the solar atmospheric curve needs to be removed, otherwise the lowest value in the 2000- to 2400-nm region will occur at the longest wavelength. To correct for these effects, the hull quotient technique was applied to log residual data. Both these techniques are described in Green and Craig (1985). The wavelength, depth full width half maximum of the deepest feature, was then extracted from the hull quotients of the log residual data. The wavelength of the deepest feature was displayed as a gray level (dark - short wavelengths; light - long wavelengths). The depth of this feature was also displayed as a gray level (dark, deep feature; light, shallow feature). Wavelength and depth images for the study area are shown in Figure 5/Slide 21. The wavelength image is particularly useful for separating the alteration types. The area mapped as buddingtonite appears dark having an absorption feature at the shortest wavelengths (2120 nm). The area mapped as alunite appears slightly lighter since its deepest absorption feature is around 2170 nm. The kaolinite area appears lighter still, its deepest absorption feature occurring around 2209 nm. The silicified area appears lightest, its deepest absorption feature occurring around 2250 nm.

Using the decorrelation stretch, log residual, and WDW images, it was possible to produce an mineralogic map of the area (Figure 6). It should be realised that this map is only a first attempt; nonetheless, it does improve on certain aspects of the existing alteration map. For example, the silicified area has been separated into an outer and inner silicified zone. The opalised and argillised zones, which are often difficult to separate on the ground, have been divided according to the dominant alteration mineral present, either alunite, buddingtonite, or kaolinite.

SUMMARY AND CONCLUSIONS

The 1989 AVIRIS data are capable of differentiating areas rich in the alteration minerals alunite, buddingtonite, kaolinite, and silica at Cuprite, Nevada. This can be achieved using a color composite generated from a decorrelation stretch of three AVIRIS channels selected to maximise differences in the spectral shapes of these minerals. However, in order to identify a particular mineral by matching the absorption features in the AVIRIS spectrum with those in the laboratory spectrum of a pure mineral, further processing is required to remove a series of systematic effects superimposed on the spectrum of the surface material. These relate to the solar irradiance curve, atmospheric absorption/ scatter, and topographically induced illumination differences. These can be adequately removed using the log residual calculation. After removal of these effects, spectra from five areas in the image clearly matched laboratory spectra obtained from field samples collected from those areas. Particularly noteworthy was the well-defined kaolinite doublet in the AVIRIS spectra. The ability to resolve this doublet may permit the separation of areas of kaolinite from dickite,

which can be distinguished in laboratory spectra in this wavelength region by a subtle difference in the shape of this doublet.

A further technique that proved particularly useful for identifying the dominant alteration mineral in an area involved searching for the wavelength, depth and full width half maximum of the deepest absorption feature and displaying these three pieces of information as separate gray-scale images.

Using the decorrelation stretch, log residual, and WDW data, it was possible to produce a mineralogic map of the area that was then compared to an existing alteration map. The mineralogic map concurred with the existing alteration map and permitted greater separation of certain units. For example, the previously mapped silicified zone was separated into an outer and inner silicified zone.

ACKNOWLEDGMENTS

The research described in this paper was carried out whilst the first author held a National Research Council, Resident Research Associateship at the Jet Propulsion Laboratory, California Institute of Technology.

REFERENCES

Abrams, M. J., Ashley, R. P. 1980. *Alteration Mapping Using Multispectral Images - Cuprite Mining District, Esmeralda County, Nevada. U.S. Geological Survey* Open File Report 80-367.

Buchanan, L. J., 1981. Precious Metal Deposits Associated With Volcanic Environments in the Southwest. In *Relations of Tectonics to Ore Deposits in the Southern Cordillera*, eds. W. R. Dickinson and W. D. Payne (*Arizona Geological Society Digest,* v. 24), pp. 237-262.

Gillespie, A. R., Kahle, A. B., Walker, R. R., 1986. Color Enhancement of Highly Correlated Images: I Decorrelation and HSI Contrast Stretches. *Remote Sensing of Environment.* v. 20, pp. 209-235.

Goetz, A. F. H. and Srivastava, V., 1985. Mineralogic Mapping in the Cuprite Mining District. *Proceedings of the First AIS Workshop.* Publication 85-41, Jet Propulsion Laboratory, Pasadena, California.

Goetz, A. F. H., Rock, B. N., Rowan, L. C., 1983. Remote Sensing for Exploration: An Overview. *Economic Geology*, 78, pp. 573-590.

Green, A. A., and Craig M. D., 1985. Analysis of Aircraft Spectrometer Data With Logarithmic Residuals. *Proceedings of the First AIS Workshop.* Publication 85-41, Jet Propulsion Laboratory, Pasadena, California.

Krohn, M. D. and Altaner, S. P., 1987. Near-Infrared Detection of Ammonium Minerals. *Geophysics.* v. 52, pp. 924-930.

Kruse, F. A., Calvin, W. M., Seznec, O., 1988. Automated Extraction of Absorption Features From Airborne Visible/Infrared Imaging Spectrometer (AVIRIS) and Geophysical and Environmental Research Imaging Spectrometer (GERIS) Data. *Proceedings of the AVIRIS Performance Evaluation Workshop.* Publication 88-38, Jet Propulsion Laboratory, Pasadena, California, pp.62-75.

Kruse, F. A., Kierein-Young, K. S., Boardman, J. W., 1990. Mineral Mapping at Cuprite, Nevada With a 63-Channel Imaging Spectrometer. *Photogrammetric Engineering and Remote Sensing.* v. 56, pp. 83-92.

Murray, H. H., 1988. Kaolin Minerals: Their Genesis and Occurrences. In *Hydrous Phyllosilicates,* ed. S. W. Bailey (*Reviews in Mineralogy,* Mineralogical Society of America v. 19), pp. 69.

Podwysocki, M. H., Salisbury, J. W., and Vergo, N., 1985. Use of Near-Infrared Spectra to Distinguish Between Sedimentary Cherts and Hydrothermal Silica Associated With Disseminated Gold Deposits. Geological Society of America, Abstract.

Roberts, D. A., Yamaguchi, Y., Lyon, R. J. P., 1985. Comparison of Various Techniques for Calibration of AIS Data. *Proceedings of the Second AIS Data Analysis Workshop*. Publication 86-35, Jet Propulsion Laboratory, Pasadena, California, pp. 21-30.

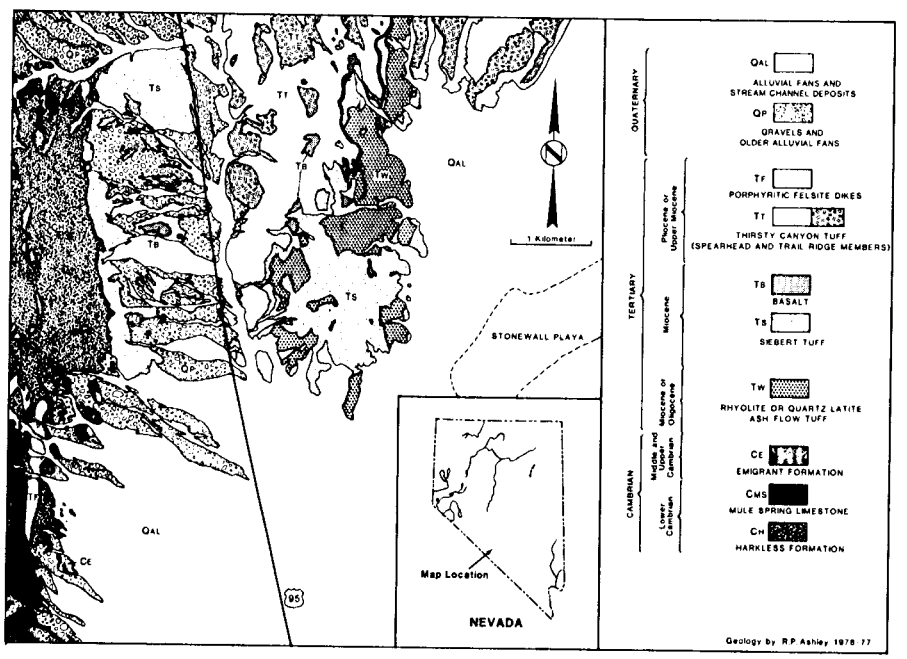

Figure 1. Geologic map of the Cuprite, Nevada study site. Redrawn from Ashley and Abrams (1980).

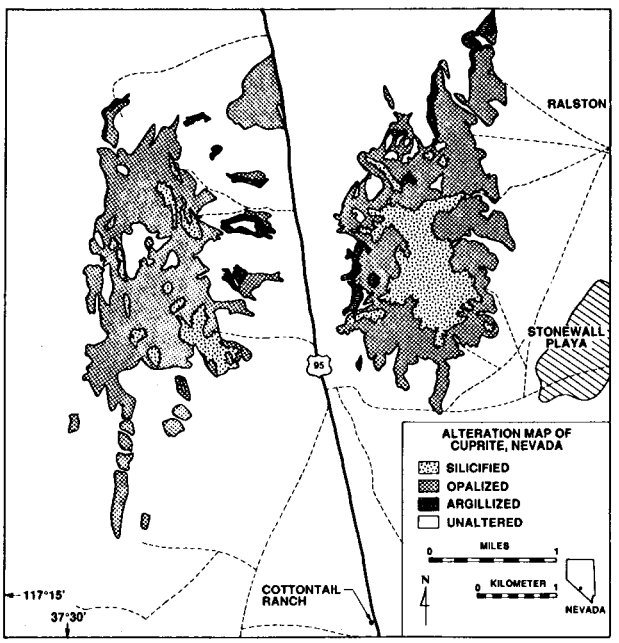

Figure 2. Alteration map of the Cuprite, Nevada study site. Redrawn from Ashley and Abrams (1980).

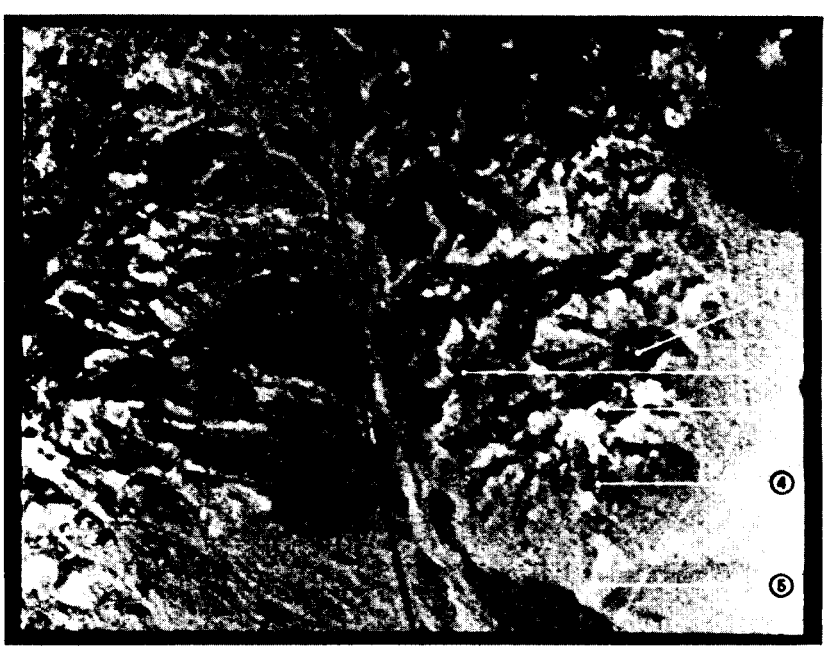

Figure 3. Color composite image produced from a decorrelation stretch of AVIRIS bands 187 (2088 nm), 192 (2134 nm),and 198 (2217 nm) displayed as red, green, and blue, respectively.

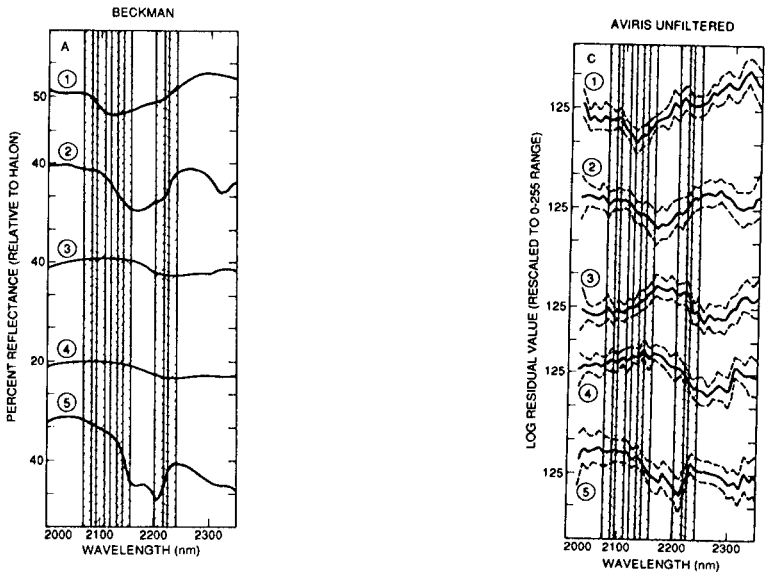

Figure 4. Laboratory and AVIRIS SWIR spectra for five sites at Cuprite. The AVIRIS spectra are the result of a log residual algorithm applied to the entire flight line.The spectra are offset for clarity; 1=Buddingtonite Zone, 2=Alunite Zone, 3=Silicified Zone edge, 4=Silicified Zone center, 5=Kaolinite Zone.

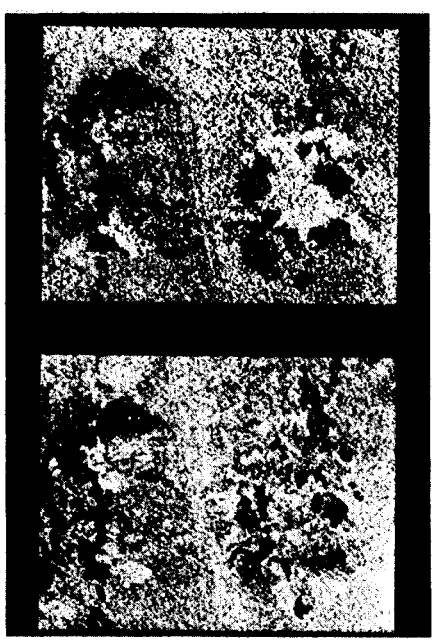

Figure 5. Wavelength and depth of deepest absorption feature in each pixel in hull quotients of log residual AVIRIS data from 2000 to 2350 nm wavelength range displayed as gray scale images. Wavelength - top; depth - bottom.

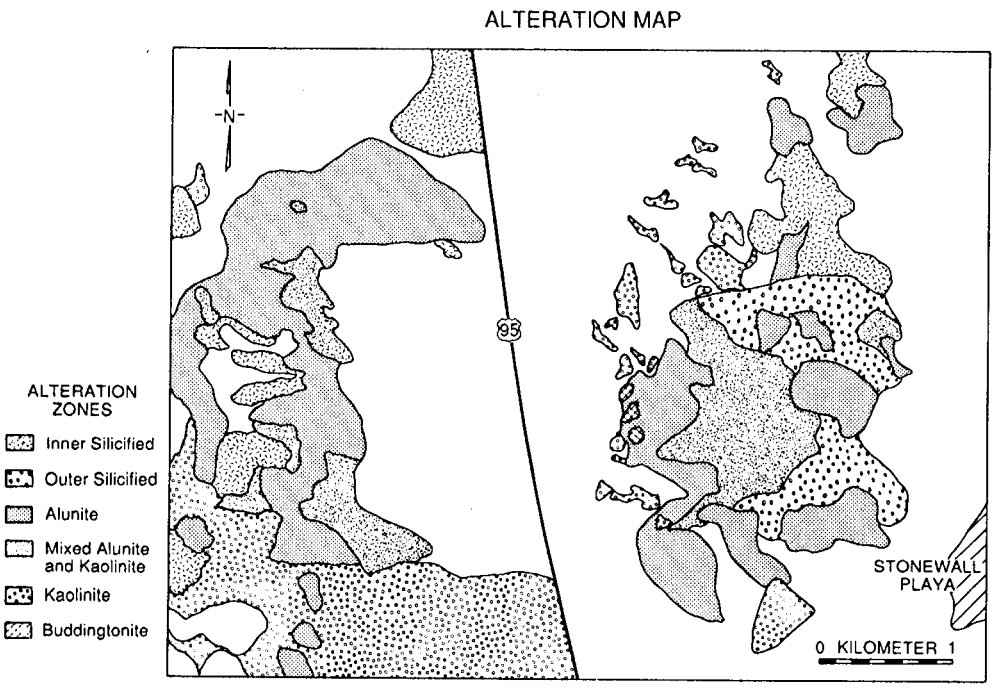

Figure 6. Simplified alteration map of the Cuprite, Nevada study site from analysis of AVIRIS SWIR data.